Heritage Science

RESEARCH

Open Access

Spatiotemporal evolution of landscape stability in World Heritage Karst Sites: a case study of Shibing Karst and Libo-Huanjiang Karst

Xue Bai[1], Kangning Xiong[1*], Yue Chen[1] and Ziqi Liu[1]

Abstract

Landscape stability is a paramount concern within the field of landscape ecology. Indices of landscape patterns not only facilitate an effective analysis of land use transformations but also delve into the mechanisms of landscape disturbances across various spatial and temporal dimensions. Utilizing land use data spanning from 2014 to 2022 for the Shibing and Libo-Huanjiang South China Karst (SCK) World Heritage Sites (WHSs), this study delves into the landscape dynamics of these areas over the past 8 years. This investigation employs landscape pattern indices and a moving window technique to construct a landscape stability evaluation model, incorporating indices such as the Contagion Index, Patch Density, and Total Edge Contrast. Moreover, the study employs Moran's I, a spatial autocorrelation index, to scrutinize the shifts in geographical heterogeneity of landscape stability within the said period. The findings reveal: (1) Between 2014 and 2022, the landscape patterns of the Shibing and Libo-Huanjiang WHSs have undergone significant transformations, with Woodland emerging as the predominant landscape type and its area exhibiting an upward trend in recent years. (2) The level of fragmentation within the research area has decreased, landscape diversity has diminished, and the aggregation index has risen, according to the landscape pattern indices from 2014 to 2022, indicating that conservation measures have significantly influenced the evolution of landscape patterns. (3) Throughout most of the study period, landscape stability predominantly remained at a relatively stable level, albeit with noticeable fluctuations in years heavily impacted by human activities. (4) The areas of high-high agglomeration and the hotspots of the heritage sites were primarily concentrated within the core zones of these sites, suggesting focused areas of conservation and landscape integrity.

Keywords Landscape pattern, Spatiotemporal changes, Landscape stability, South China Karst, World heritage site

Introduction

Ecosystem stability is defined as the ability of an ecosystem to maintain or restore its structure and function to relative stability [1]. The stability of an ecosystem is influenced by ecosystem or landscape characteristics, which are prerequisites for the normal functioning of the ecosystem. These comprise biodiversity-related factors, species features, ecosystem functions (like feedback and modular structures), and landscape indicators (like connectedness and fragmentation) [2]. Landscape stability can be seen as a reflection of ecosystem stability on a larger spatial scale. It considers the relationships and stability between ecosystems as well as between ecosystems and their surrounding environment, in addition to the stability within ecosystems. Experts in historical land use change define "landscape stability" as the constancy of land use polygons [3]; Researchers view landscape resilience, persistence, and resistance to disturbance as a collective concept of landscape stability [4]. Landscape

*Correspondence:
Kangning Xiong
xiongkn@163.com
[1] School of Karst Science, Guizhou Normal University / State Engineering Technology Institute for Karst Desertification Control, 116 Baoshan North Road, Guiyang 550001, Guizhou, China

stability refers to the ability of a specific area or landscape to maintain its functions, structure, and biodiversity over a period of time. This concept involves factors from ecological, socioeconomic, and cultural dimensions. It emphasizes the landscape's ability to maintain its core characteristics and service functions in the face of external changes, such as climate change, population growth, and land use changes [5]. Research on landscape stability contributes to the understanding of how ecosystems respond to natural and anthropogenic disturbances on a larger scale, and how they maintain and develop their ecological services and processes. It is crucial for understanding and conserving both natural and cultural landscapes. However, at present, most scholars focus on the stability of landscapes in urban areas, wetlands, basins, and the stability of ecosystems in WHSs [6, 7], with relatively little attention given to the landscape stability of heritage sites. The impact of natural and human factors on heritage sites over time is difficult to perceive and quantify. Since the preservation of natural heritage is closely related to the stability of heritage landscapes, studying landscape stability is essential to creating more efficient management and planning techniques. This is not only important for achieving a balance between environmental protection and socioeconomic development but is also particularly significant for the long-term development of heritage sites, as they frequently serve as important venues for tourism and cultural education.

Landscape pattern generally refers to the spatial morphological organization of landscapes, which has certain structural characteristics and can reveal the underlying processes of change [8]. To comprehend the dynamics of pattern-process at particular scales, dynamic evolution analysis mainly focuses on the composition and configuration of landscapes, examining the patterns of landscape change in particular areas [9]. Strictly speaking, the foundation of landscape ecological planning is the link between landscape patterns and spatial processes in landscape ecology [10]. Achieving regional sustainable development, improving ecological functions that are in danger of being lost, enhancing landscape connectivity, harmonizing ecological processes among spatial elements, and optimizing spatial elements like area, shape, type, and configuration are the main goals of human spatial pattern planning and management [11].

The strength of the relationship that exists between humans and the environment differs from person to person and from landscape to landscape, which has an impact on both society and the composition and functionality of ecosystems. Humans and environments can create a "malignant" or "benign" cycle through their interaction. Creating a positive feedback loop between socioeconomic factors and ecosystems in the landscape can be effectively achieved by connecting humans with nature [12]. The stability and balance of a landscape can be considered as a function of disturbance on a relative spatiotemporal scale, determined by the frequency and intensity of disturbances and the ecological characteristics of the landscape [13]. Research on landscape patterns can quantitatively explore the internal laws of landscapes, analyze factors affecting landscape patterns, evaluate landscape types, and then propose optimization measures. Combining landscape indices to analyze the landscape patterns of specific areas is beneficial for promoting the sustainable development of landscape science, advancing land planning, and establishing sustainable human settlements [14].

With carbonate rocks making up almost 13% of the nation's total land area, China is among the nations with the greatest distribution of these rocks worldwide. The SCK region covers 500,000 km^2 and is mainly made up of the provinces of Yunnan, Guizhou, and Guangxi. It also includes portions of Chongqing, Sichuan, Hunan, Hubei, and Guangdong. For a variety of karst landforms in humid-semi-humid, tropical-subtropical plains, hills, mountains, and plateaus, this region is the best-developed area in the world. It captures the distinct natural geographic conditions and history of geological evolution seen in the majority of regions in China. The unique karst topography, karst ecosystems, biodiversity, scenic beauty, and evolutionary processes—many of which have worldwide significance—that define the SCK are its defining features. South China offers the most variety of karst landscapes and features [15]. The SCK WHSs are "outstanding examples reflecting major stages of Earth's evolutionary history, including the record of life, significant ongoing geomorphic processes, significant geomorphological forms, or natural geographic features." Including the Karst regions of Guilin, Huanjiang, Wulong, Jinfoshan, Shibing, Libo, and Shilin, these seven Karst heritage sites authentically and collectively show the entire sequence of the development and evolution of tropical and subtropical Karst from young to old, from plateau mountains to low hills. They have a fascinating historical background in addition to great scientific significance.

The Shibing WHS is distinguished by its subtropical dolomite landscape, which represents a rare type of spectacular conical peak-cluster and gorge karst developed on pure, thick, and ancient dolomite, filling a gap in the types of SCK. It is composed of pure white Cambrian dolomite, with soils primarily consisting of thin layers of dolomitic limestone weathered from the dolomite. Due to its inherent fragility, it is highly susceptible to the impacts of the climatic environment. With the rise of tourism, there has been excessive development and utilization of the karst

landscape. Continuous changes in the climate and human activities have caused varying degrees of damage to both the karst landscape and its ecosystem.

The Libo-Huanjiang WHS has unique conical karst, which is the most typical of peak-cluster and peak-forest karst and serves as a paradigm of similar landforms worldwide [16]. It is not only a world-class example of peak clusters but also a typical representative of conical karst in the moist tropical-subtropical interiors of continents. The soil is mainly neutral to slightly alkaline limestone soil, among which, the black limestone soil developed under the karst peak forests, peak clusters, and slopes of karst valleys is the most common. Additionally, some yellow soils are distributed in karst depressions, basins, and valley bottoms. The growth of trees is severely hindered by the karst ecological conditions characterized by shallow soil, discontinuous soil cover, limited space for rooting, and drought, making forest vegetation difficult to recover once destroyed.

Extending current study theories, the research on Shibing SCK and Libo-Huanjiang SCK has great scientific value. Theoretical findings also apply to other South China Karst WHSs. Furthermore, WHS ecosystems are often among the best in the world for ecological quality. Because of this, the developed landscape structure and stability evaluation models can be applied to other similar heritage conservation areas, providing valuable guidance for the preservation of the environment and ecology in other locales and encouraging the growth of a sustainable regional economy in the Karst WHS of Southern China. Analyzing their landscape stability might help promote peaceful cohabitation between humans and the natural environment by serving as a model for global ecosystems [17–19].

Materials and methods

Study area

The Shibing WHS is situated on a slope that crosses over from the western Hunan hills to the central Guizhou mountains in Shibing County, eastern Guizhou Province (Fig. 1). It is a component of the Yangtze River basin, which also includes the Waqiao, Shanmu, and middle

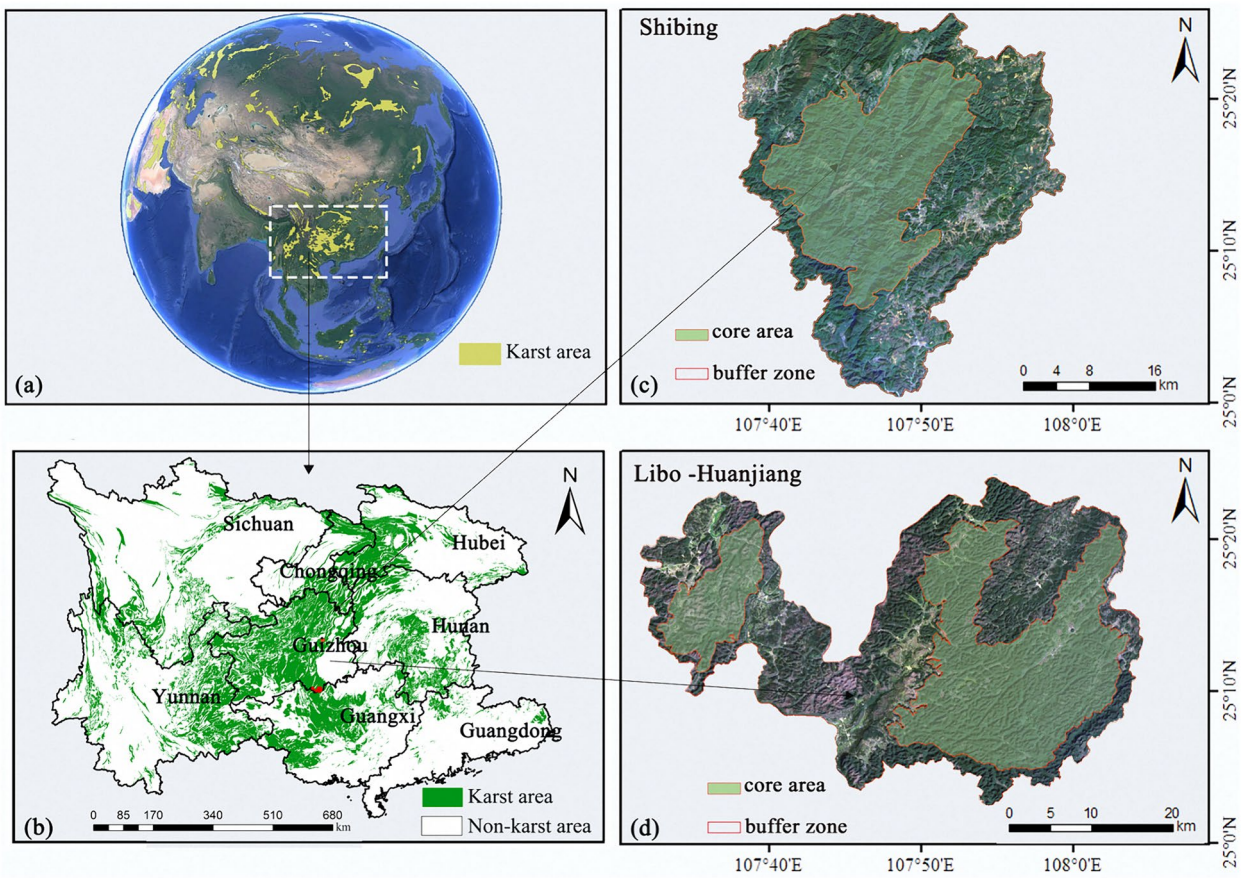

Fig. 1 **a** Karst Distribution in the Northern Hemisphere; **b** Location of the SCK; **c** Satellite imagery of Shibing WHS in 2022; **d** Satellite imagery of Libo-Huanjiang WHS in 2022

Wuyang Rivers. The Wuyang River is a tributary of the Yuanjiang River system. The Wuyang River and its tributary, the Shanmu River, constitute the regional erosional-karst base level, which is essential to the hydrodynamic structuring of the Karst topography. The region has developed surface water. The Shibing Karst WHS spans 102.80 km^2 in total. With an average elevation of 912 m and most places between 600 and 1250 m, the terrain is higher in the north and lower in the south. The geological backdrop of dolomite dominates the northern tributaries, which converge southward. Strong river erosion has produced an amazing gorge Karst landscape and peak cluster [16, 19].

The Libo-Huanjiang WHS is situated near the boundary of Huanjiang County in Hechi City, Guangxi Zhuang Autonomous Region, and Libo County in Qiannan Prefecture, Guizhou Province. The Guangxi Mulun National Nature Reserve, the Zhangjiang National Beautiful Area including the Daqikong and Xiaoqikong beautiful places, and the Guizhou Maolan National Nature Reserve make up the majority of the heritage site. With a buffer zone of 434.98 km^2 and a core area of 295.18 km^2, the Libo Heritage Site has a total area of 730.16 km^2. With an average elevation of 747 m, the altitudes vary from 385 to 1109 m. From north to south, the land gradually descends from high points in the west to low points in the east, where it eventually joins the Guangxi Basin. Its characteristic conical Karst and mix of surface and subsurface Karst ecosystems define it. With a core area of 71.29 km^2 and a buffer zone of 44.43 km^2, the Huanjiang WHS has a total area of 115.59 km^2. The development, evolution, and distribution integrity of the Libo conical Karst landscape are greatly enhanced by the Huanjiang Karst, which is an extension of the Southern China Karst Libo Karst WHS. It is an exceptional example of tropical and subtropical conical Karst together with the Libo Karst [19].

Date and processing

The study obtained Landsat 8 OLI satellite remote sensing images for the years 2014, 2018, and 2022 covering both study areas, sourced from the Geospatial Data Cloud (https://www.gscloud.cn/) and the United States Geological Survey (USGS) (https://earthexplorer.usgs.gov/). Multi-band image synthesis and geometric corrections were conducted in ENVI (Exelis Visual Information Solutions, Melbourne, Florida, USA; version 5.2). The image classification system referenced the "Current Land Use Classification" (GB/T21010-2017) standards. Considering the specific conditions of the study area and based on the attributes of land resources and their utilization, the areas were classified into six categories (Table 1): cultivated land, woodland, grassland, water bodies, built-up land, and unused land. Vector data of land use spatial distribution for the three periods were obtained through interpretation combined with field surveys.

Research methods

A fundamental component of landscape ecology is the connection between ecological processes and landscape patterns. Landscape pattern indices establish a connection between landscape patterns and their evolutionary processes by measuring the landscape structure and its dynamics [20]. Landscape pattern indices encompass most information about regional landscape patterns, reflecting the composition and spatial configuration of landscape structures, clearly expressing the types and arrangement of landscape units within a region, and indicating landscape spatial heterogeneity [21, 22]. The study uses data from transition matrix computations to examine changes in the landscape structure in the area during the past eight years based on the research objectives and the actual landscape of the Shibing and Libo-Huanjiang WHSs. To represent the spatiotemporal evolution of landscape patterns and shifts in ecological processes in the research area, twelve landscape pattern indices are chosen, one at the patch-type level and one at the overall landscape level. For a more accurate quantitative analysis of the spatial distribution characteristics of landscape stability changes, local operation methods are employed. A landscape stability evaluation model is built to measure the spatiotemporal distribution characteristics and trends of landscape stability changes.

Table 1 Classification of landscape types

Landscape types	Meaning
Cultivated land (CL)	Areas designated for the cultivation of agricultural crops
Grassland (GL)	Areas primarily covered with herbaceous plants, with a coverage of more than 5%. This includes grasslands primarily used for grazing, shrub grasslands, and sparse woodlands with a canopy closure of less than 10%
Woodland (WL)	Areas used for growing trees, shrubs, bamboo, and other plants for forestry purposes
Waterbody (WB)	Areas comprising natural land water bodies and lands designated for water management and conservancy infrastructure
Build-up land (BL)	Residential areas in villages and lands used for industrial, mining, and transportation purposes outside these settlements
Unused land (UL)	Land that is currently not in use, including areas that are difficult to utilize or develop

Landscape transition matrix

One quantitative way to describe changes between states is with a transition matrix. The landscape type transition matrix efficiently illustrates the changes that occur between various landscape types, highlighting the structural features of the terrain as well as the reciprocal changes and directions that occur between various landscape types [23, 24]. This study uses the landscape transition matrix to investigate the inter transformation of various landscape types within WHSs. The mathematical form of the transition matrix is as follows:

$$S_{ij} = \begin{bmatrix} S_{11} & S_{12} & \ldots & S_{1n} \\ S_{21} & S_{22} & \ldots & S_{2n} \\ \ldots & \ldots & \ldots & \ldots \\ S_{n1} & S_{n2} & \ldots & S_{nn} \end{bmatrix} \quad (1)$$

where S_{ij} represents the area of landscape type i at the starting period that transforms into landscape type j at the end period; n is the number of landscape types.

Landscape pattern indices

Landscape pattern indices are a comprehensive study and quantitative reflection of various characteristics of landscapes, highly concentrating information about landscape patterns. They effectively reflect the composition and spatial configuration of landscape structures and also indicate the spatial characteristics of the landscape and the impact of human or natural factors on ecological processes at different scales, making them a classic method for describing landscape patterns and their changes [25–27]. Even though each landscape measure emphasizes ecological relevance differently, several indices frequently show a significant amount of association with one another. Thus, it is possible to make sure that the chosen indices represent non-redundant landscape information by computing the correlation coefficients between landscape indices and running correlation tests under specified confidence requirements. This method avoids the problem of index redundancy in landscape ecological evaluations while accurately describing landscape patterns and reflecting the relationship between processes and landscape patterns.

Two criteria are used to pick landscape indices: the patch-type level, which reflects characteristics of the land use landscape pattern, and the landscape type level. At the patch-type level, the selected indices include Patch Number (NP), Patch Density (PD), Largest Patch Index (LPI), Landscape Shape Index (LSI), and Aggregation Index (AI). At the landscape type level, indices such as Patch Density (PD), Interspersion and Juxtaposition Index (IJI), Division Index (DIVISION), Total Edge Contrast Index (TECI), Splitting Index (SPLIT), Shannon's Diversity Index (SHDI), Shannon's Evenness Index (SHEI), and Contagion Index (CONTAG) are chosen, making a total of 12 landscape indices to analyze landscape pattern changes. The statistical properties and ecological implications of these indices are detailed in Table 2.

Landscape stability evaluation method

The stability of a landscape is contingent upon the stability of its various patch types and the ability of the landscape's compositional structure to sustain the continuity and stability of ecological processes and functions. Therefore, the evaluation of landscape stability can be conducted by measuring the relationship between changes in the spatial structure and stability of regional patches. In this study, based on the principles of hierarchical patch dynamics theory, we employed the Spearman rank correlation method to select landscape indices with low intercorrelation to construct a model for evaluating landscape stability [20]. We identified three indices to construct the landscape stability evaluation model: contagion, total edge contrast, and patch density. The contagion index primarily reflects the spatial configuration characteristics of landscape components and the continuity of a dominant landscape type, serving as an important indicator for measuring the spatial aggregation characteristics of landscape patch types. The patch density and total edge contrast indices directly reflect the degree of fragmentation and spatial heterogeneity of the landscape, which to some extent indicate the degree of human disturbance on the landscape [14, 23, 28, 29]. The formula for calculating landscape stability is as follows:

$$S = \frac{C}{P^{*}T} \quad (2)$$

where S represents the landscape stability index; C is the Contagion Index (CONTAG); P is the Patch Density (PD); T is the Total Edge Contrast Index (TECI). When using TECI, it is necessary to first determine the edge contrast weight between different landscape types. The setting of this weight follows these principles (Table 3): hard boundaries (cultivated land, build-up land) and soft boundaries (woodland, grassland, unused land) > hard boundaries and neutral hardness boundaries (water bodies) > soft boundaries and soft boundaries. This paper refers to the studies by Wang Zhiqiang et al. [20, 23, 30]. for setting these weights, as shown in Table 3. The higher the Contagion Index (CONTAG), and the lower the Patch Density (PD) and Total Edge Contrast Index (TECI), the higher the stability of the landscape pattern, and the stronger the landscape's resistance to external disturbances.

Table 2 Selection of landscape pattern indices and their ecological significance

Index nature	Landscape Index name	Ecological significance
Patch type level	Patch Number (NP)	Indicates the total number of patches in the landscape, related to landscape fragmentation; higher values indicate higher fragmentation
	Patch Density (PD)	Reflects fragmentation of the landscape and the fragmentation degree of a certain type; higher density indicates more severe fragmentation
	Largest Patch Index (LPI)	Indicates the influence of the largest patch on the entire type or landscape; its value change can reflect the variation in human disturbance intensity
	Landscape Shape Index (LSI)	Reflects the complexity of patch shapes in the landscape pattern; higher values indicate greater complexity
	Aggregation Index (AI)	Reflects the aggregation degree of each attribute grid in raster format data, assessing the connectivity between patches of each landscape type
	Patch Density (PD)	Reflects the overall heterogeneity and fragmentation of the landscape; higher density indicates more severe fragmentation
	Interspersion & Juxtaposition Index (IJI)	Measures the overall distribution and adjacency of patch types
	Division Index (DIVISION)	Assesses the degree of separation of the same patch type, with smaller values indicating greater dispersion
Landscape type level	Total Edge Contrast Index (TECI)	Describes the contrast of landscape boundaries, with higher contrast approaching
	Contagion Index (CONTAG)	Describes the degree of non-randomness or aggregation of different patch types in a landscape
	Fragmentation Degree (SPLIT)	Quantifies the fragmentation level of a landscape, with values ≥ 1. Higher values indicate greater fragmentation
	Shannon's Evenness Index (SHEI)	Represents the evenness of distribution across different landscape types
	Shannon's Diversity Index (SHDI)	Reflects landscape diversity, where higher values indicate richer diversity

Table 3 Setting of edge contrast weight

	CL	WL	GL	WB	BL	UL
CL	0	0.8	0.8	0.6	0.3	0.8
WL	0.8	0	0.1	0.5	0.8	0.1
GL	0.8	0.1	0	0.5	0.8	0.1
WB	0.6	0.5	0.5	0	0.6	0.5
BL	0.3	0.8	0.8	0.6	0	0.8
UL	0.3	0.1	0.1	0.5	0.8	0

The study uses the moving window method for visual analysis of landscape stability. The fuzzy membership function is used for normalization, and then the natural break method is applied to classify landscape stability into five levels: unstable, relatively unstable, relatively stable, stable, and extremely stable [29, 30].

Spatial autocorrelation analysis

One popular technique for examining the spatiotemporal pattern evolution of regional variables is spatial autocorrelation analysis. It is employed to examine the patterns of components' spatial distribution, which are commonly quantified by Moran's index and comprise both local and global spatial autocorrelation. To more intuitively illustrate spatial clustering, local spatial autocorrelation analysis (LISA index) identifies specific aggregation areas of characteristics in geographical space and is analyzed using the spatial association index Getis-Ord G_i^*[31, 32].

Global spatial autocorrelation analysis (Moran's I index) can determine the overall spatial distribution, and its formula is as follows:

$$I = \frac{n\sum_{i=1}^{n}\sum_{j=1}^{n} W_{ij}(x_i - \overline{x})\left(x_j - \overline{x}\right)}{\sum_{i=1}^{n}\sum_{j=1}^{n} W_{ij}\sum_{i=1}^{n}(x_i - \overline{x})^2} \tag{3}$$

where I represent the global Moran's I index, n is the number of spatial regions, x_i and x_j are the attribute values of the geographic units in regions i and j respectively, W_{ij} is the spatial weight matrix between features i and j, and $\bar{x}$ is the average value of the attributes across all regions. The range of Moran's I index is [− 1, 1]; when Moran's I index is close to − 1, it indicates a more significant negative spatial autocorrelation; when Moran's I index is close to 1, it indicates a more significant positive spatial autocorrelation; when Moran's I index is 0, it indicates the absence of spatial autocorrelation.

Local spatial autocorrelation analysis decomposes the global spatial autocorrelation Moran's Index into individual units, to examine whether there is local spatial clustering in specific regions. The formula is as follows:

$$I_i = \frac{x_i - \bar{x}}{S^2} \sum_{j=1}^{n} W_{ij}\left(x_j - \bar{x}\right) \tag{4}$$

where I_i represents the local Moran's Index. When I_i is positive, it indicates a spatial cluster of high–high or low–low values around the regional unit. When I_i is negative, it indicates a spatial cluster of high–low or low–high values around the regional unit. S^2 represents the variance of the landscape stability index. In this article, the LISA results are categorized into five classes: high–high (H–H), low–low (L–L), high–low (H–L), low–high (L–H), and not significant.

Hotspot analysis is used to study the degree of clustering of different attribute values, where hotspot areas represent the clustering of high values, and cold-spot areas represent the clustering of low values. Getis-Ord G_i^* analysis is a local spatial autocorrelation index based on distance matrices used to explore the spatial clustering locations of high or low values of various factors [32, 33], and its formula is as follows:

$$G_i^* = \frac{\sum_j^n W_{ij} x_j}{\sum_j^n x_j} \tag{5}$$

where x_j and W_{ij} have the same meanings as defined in the formula (3).

Results

General characteristics of landscape transition

General characteristics of landscape transition in Shibing World Heritage Site

According to Fig. 2, the landscape types that dominated the Shibing WHS between 2014 and 2022 were WL and CL, which combined accounted for more than 80% of the total area. While BL and CL were detected in the buffer zone, WL was mostly found in the Shibing Karst's core area. Distributions of WB and UL were rather consistent. In the studied area, WL dominated the landscape type and had a distinct distribution advantage. The proportion of the six types of landscapes in the study region in 2014, 2018, and 2022, in descending order of area, were WL, CL, GL, BL, UL, and WB, according to the data results.

In 2008, the study area was prepared for the World Heritage application, and on June 23, 2014, at the 38th

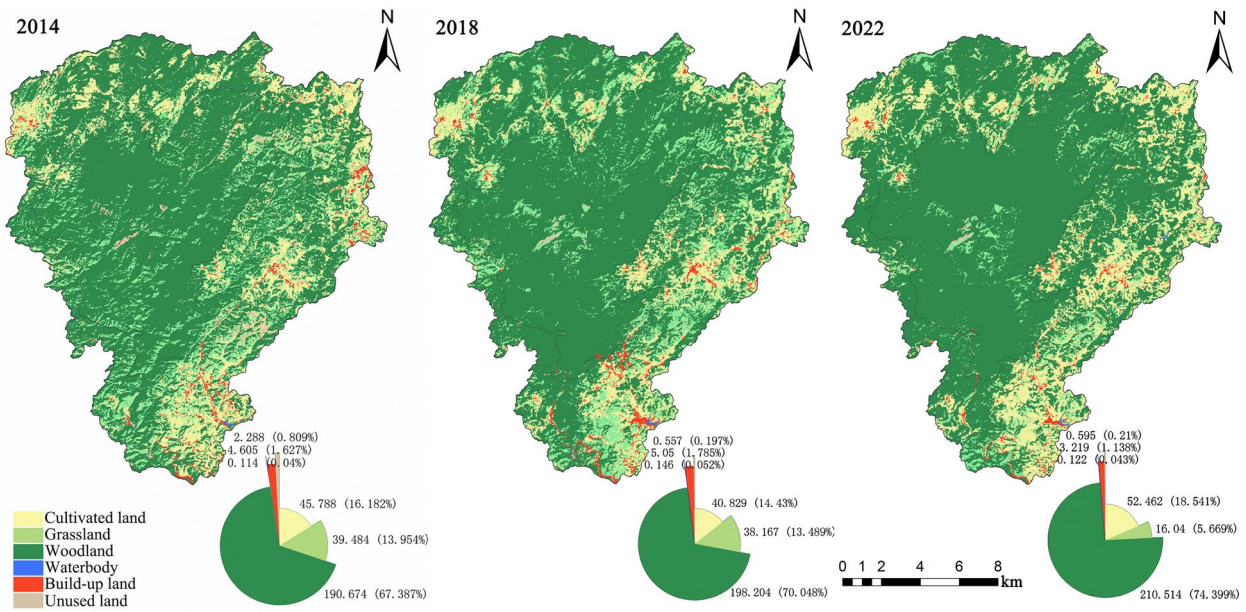

Fig. 2 Spatial distribution and area proportion of landscape types in Shibing WHS

session of the World Heritage Committee held in Doha, Qatar, the application for the second phase of the SCK was approved, with Yuntai Mountain in Shibing, Guizhou representing the project. Yuntai Mountain became the third World Natural Heritage site in Guizhou Province. During this process, it was inevitable to reduce human traces in the area and conduct corresponding planning. Future tourism development will require control over the distribution and quantity of human traces, such as constructed lands in the region [34].

The research area's landscape changes between 2014 and 2018 revealed seasonal variations in GL, a decline in CL, an increase in WL and BL, and a generally steady WB. Except for the northern part of the core area, landscape-type transitions were widespread throughout the research area (Fig. 3). The main alterations were between GL and WL in the Shibing WHS core area and between GL and CL in the buffer zone due to seasonal variations.

From the 2014–2018 transition matrix calculations (Fig. 4), it was found that 19.360 km^2 of GL converted to WL, 7.399 km^2 of CL to WL, and 1.648 km^2 of CL to BL. These findings demonstrate a growing appreciation for the importance of forests and the adoption of environmental conservation measures, such as reverting CL

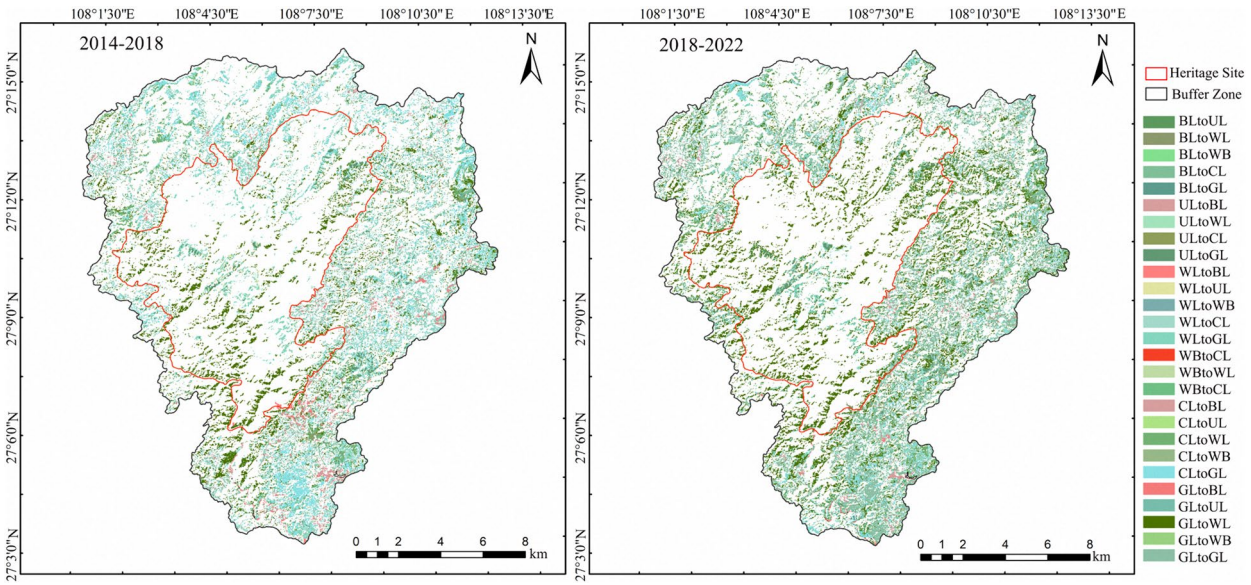

Fig. 3 Change diagram of landscape type transition in Shibing WHS from 2014 to 2022

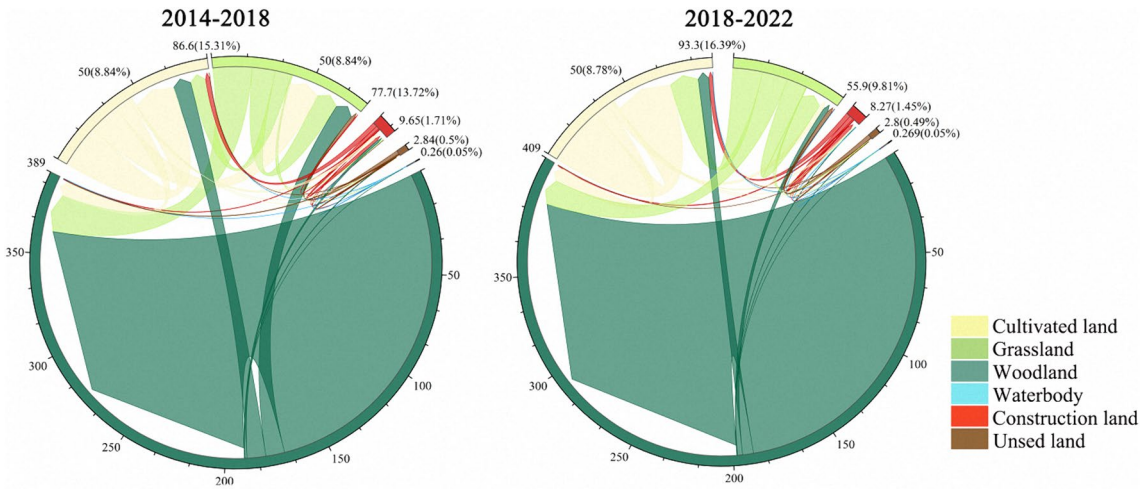

Fig. 4 Matrix chord diagram of landscape type transition in Shibing WHS

to WL. This resulted in a reduction of the CL area. The areas of CL and WL increased between 2018 and 2022, whilst the areas of WB and UL stayed mostly unchanged and BL shrank. The 2018–2022 transition matrix shows that 7.191 km^2 of CL became WL and 12.863 km^2 of GL became WL. 0.91 km^2 of CL was turned to BL. The area of cultivated land rose by 2022 as a result of Shibing County implementing the "Cultivated Land Fertility Protection Subsidy Scheme" in 2021.

General characteristics of landscape transition in Libo-Huanjiang World Heritage Site

The landscape types in the Libo-Huanjiang WHS from 2014 to 2022, as shown in Fig. 5, were primarily WL and CL, collectively making up more than 85% of the total area. While BL and CL were mostly found in the buffer zone, WL was the dominant landscape type with a clear distribution advantage, concentrated in the center of the Libo-Huanjiang WHS. The data results showed variations in the distribution of the six types of landscapes between 2014 and 2022. By 2018, UL had decreased while GL and BL had increased, with the Guiyang to Nanning Passenger Dedicated Line Railway (Guinan Railway) influencing the latter. By 2022, CL had increased and GL and UL had decreased. According to area proportion, the following landscape types were ranked in 2022: WL, CL, GL, BL, UL, and WB.

The Libo study area successfully applied for WHS in 2007, and the Huanjiang was approved during the 38th session of the World Heritage Committee held in Doha, Qatar, on June 23, 2014, as part of the second phase application for the SCK World Natural Heritage. After officially starting in 2016, the Guinan Railway's development had some effects on the buffer zone but did not immediately harm the Libo-Huanjiang Karst's conical Karst landscape or caves. Due to the construction of the Guinan Railway and the acceptance of the "Cultivated Land Fertility Protection Subsidy Scheme" in Libo County in 2021, the CL and BL area of the Libo-Huanjiang WHS grew from 2018 to 2022.

The landscape changes between 2014 and 2018 indicated a decrease in CL and UL and an increase in GL and BL, while WB and WL remained relatively stable. The landscape-type transition map (Fig. 6) shows fewer changes in the southeastern part of the study area, mainly covering the core area of Libo-Huanjiang Heritage Site, with minimal human interference.

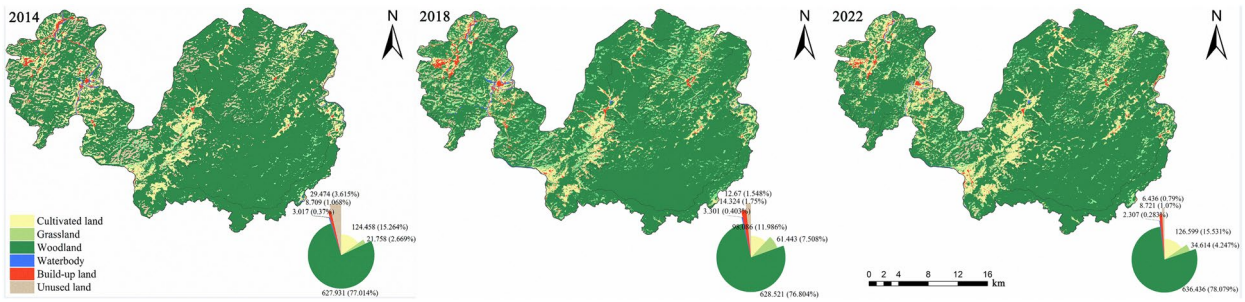

Fig. 5 Spatial distribution and area proportion of landscape types in Libo-Huanjiang WHS

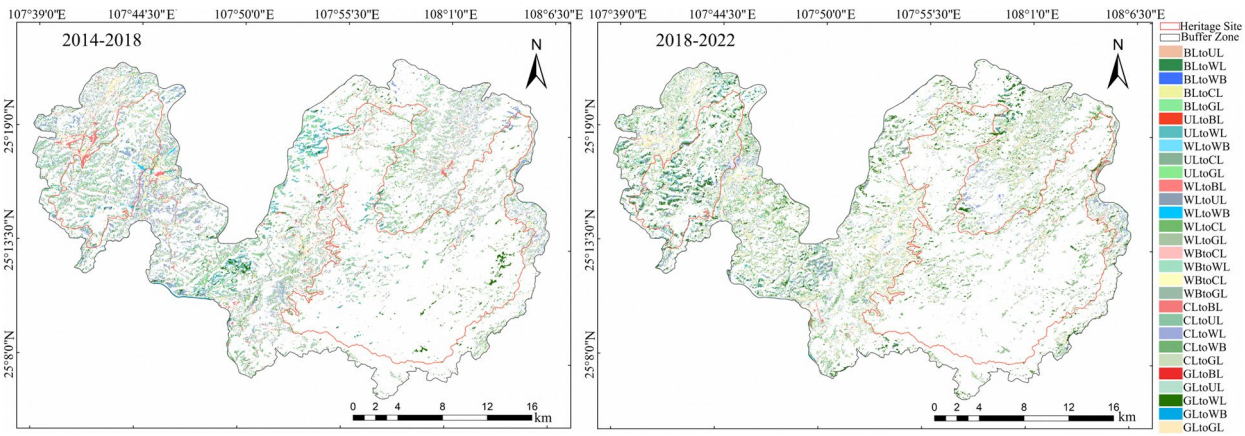

Fig. 6 Change diagram of landscape type transition in Libo-Huanjiang WHS from 2014 to 2022

The reforestation initiatives for core areas were a major factor in the transformation of CL into GL and WL, with corresponding areas of 21.985 km^2 and 33.396 km^2, according to the 2014–2018 transition matrix chord diagram. With 6.272 km^2 converted, BL grew mostly at the expense of nearby CL. The main transition from UL to GL and WL shows that desertification was well controlled. Influenced by the 2021 cultivated land protection subsidy program, CL increased between 2018 and 2022 while WB and WL stayed constant and UL and BL fell. With respective areas of 10.283 km^2 and 30.584 km^2, the landscape type area transition matrix chord diagram for 2018–2022 revealed that GL primarily transitioned to CL and WL (Fig. 7).

Dynamic changes in landscape patterns

Dynamic changes in the landscape pattern of the Shibing World Heritage Site

Table 4 shows the changes in indices for various landscape types. The number of patches (NP) for CL and GL is high, indicating that these landscapes have the highest degree of fragmentation, while the patch density (PD) values for GL, CL, BL, and WL show a declining trend, indicating that landscape fragmentation is decreasing. The largest patch index (LPI) for WL is the highest among all types, indicating that WL are concentrated and have a high degree of patch integrity, maintaining their dominance; the LPI for GL, BL, and WB initially increased and then decreased, whereas the LPI for CL

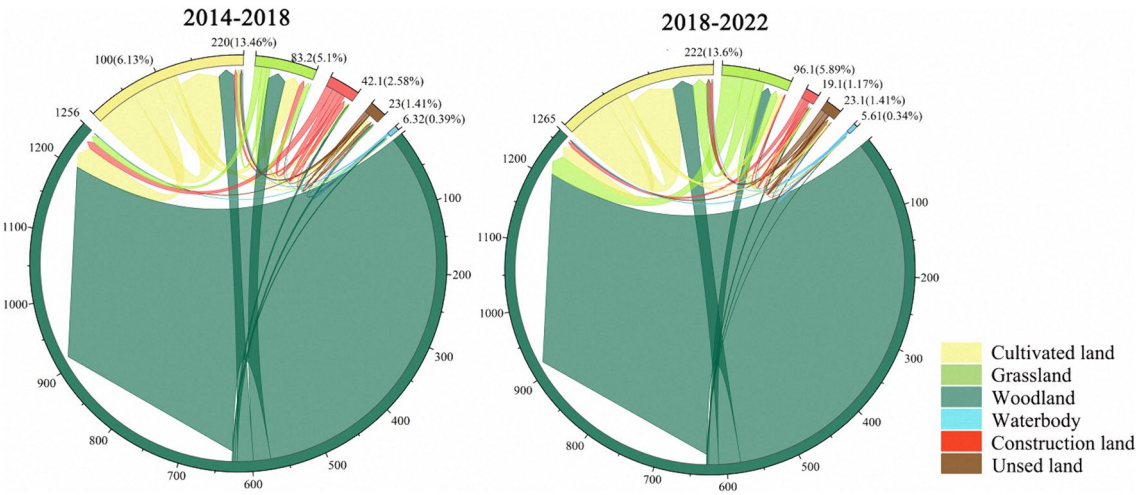

Fig. 7 Matrix chord diagram of landscape type transition in Libo-Huanjiang WHS

Table 4 Results of landscape pattern indices for different landscape types in the Shibing WHS

Patch type level	Year	GL	CL	BL	WL	WB	UL
NP	2014	7188	3749	1258	1243	36	508
	2018	5075	3004	898	1048	59	204
	2022	3329	2515	829	764	29	351
PD	2014	25.404	13.250	4.446	4.393	0.127	1.795
	2018	17.936	10.617	3.174	3.704	0.209	0.721
	2022	11.765	8.889	2.930	2.700	0.103	1.241
LPI	2014	0.226	3.106	0.106	63.589	0.019	0.071
	2018	0.652	2.567	0.159	61.964	0.025	0.024
	2022	0.090	3.996	0.077	69.222	0.019	0.057
LSI	2014	115.351	83.407	56.167	39.896	6.174	25.921
	2018	95.267	79.906	34.927	43.444	7.731	15.860
	2022	69.534	73.439	32.658	36.031	5.625	19.654
AI	2014	45.081	63.263	87.981	44.588	48.485	49.589
	2018	53.974	62.708	54.046	90.931	41.667	37.668
	2022	48.110	69.864	46.266	92.735	54.878	23.502

and UL initially decreased and then increased. This pattern depicts the effect of human activity on all six landscape types in 2018. The landscape shape index (LSI) for GL, CL, BL, and WL initially grew, then decreased. GL and CL have higher LSI values and show a decreasing trend over the study period, indicating that the irregularity of their patch shapes is greater than that of other landscape types, but this complexity has decreased over time, implying that landscape dynamic changes are moving in an ecologically favorable direction. The aggregation index (AI) for BL and UL has steadily dropped, indicating less spatial connectedness and patch aggregation. In contrast, an increasing AI value for WL indicates greater connectedness, which is good for the growth of the ecological environment.

The landscape indices at the heritage site level, as shown in Fig. 8, reveal that patch density (PD) decreased from 2014 to 2022, indicating a gradual reduction in WHS fragmentation. The fragmentation levels (SPLIT) were relatively low, indicating minimal fragmentation. The total edge contrast index (TECI) and contagion index (CONTAG) increased in the research area with time, whereas the interspersion and juxtaposition index (IJI) dropped. This shows that the landscape distribution in the research area has been unequal throughout time, with poor spatial connectedness and an increase in the intermittent and dispersed spatial distribution of landscape patches. From 2014 to 2022, the landscape division index (DIVISION) stayed largely steady. Changes in landscape heterogeneity can be assessed using Shannon's Diversity Index (SHDI) and Shannon's Evenness Index (SHEI). Between 2014 and 2018, both SHDI and SHEI gradually declined, indicating a decrease in landscape type variety. This implies that efforts were made in the development and maintenance of the heritage site to keep forests and other natural cover landscapes as dominant landscapes, in compliance with the requirements of heritage site protection and management planning, as well as tourism planning.

Dynamic changes in the landscape pattern of the Libo-Huanjiang World Heritage Site

Table 5 shows that CL and GL have a higher NP, implying that these two landscape categories are the most fragmented. WB's PD Index first drops before increasing, with a general trend toward stability. In contrast, the PD values of the other five landscape categories initially climb and later decline, indicating an overall upward trend. This implies that landscape fragmentation is increasing, and it peaked in 2018. WL's LPI Index is rather consistent, with the greatest LPI value of any landscape type during the study period. This suggests that forested areas in the study region are more concentrated and integrated, with patches consistently being the dominant kind. The LPI values of GL and BL increase and then fall, while CL decreases and then increases. UL and WB generally show a negative trend, indicating that, except for WL, other landscapes were extensively impacted by human activity throughout this time, with CL and BL being the most affected. The LSI Index for GL, CL, BL, and WL increases and subsequently drops. The high LSI values for GL and CL imply that these landscapes feature more irregularly shaped patches than other categories. The LSI values of CL and WB generally exhibit an increasing trend, indicating that the complexity and irregularity of WB patches are increasing. The steady decrease in the LSI value of UL suggests that human interference activities are becoming increasingly environmentally helpful. The AI Index for CL, BL, WL, and UL declines and then increases, although the total shift is not substantial. This demonstrates that from 2014 to 2018, as human activities increased, spatial connectedness and patch aggregation decreased, but this tendency reversed from 2018 to 2022. The GL AI value is steadily decreasing, indicating that patches are becoming more dispersed.

Figure 9 depicts the landscape indices at the landscape level of the Libo-Huanjiang WHS, which show a rising trend in the PD index from 2014 to 2018, indicating an increasing degree of fragmentation in this natural

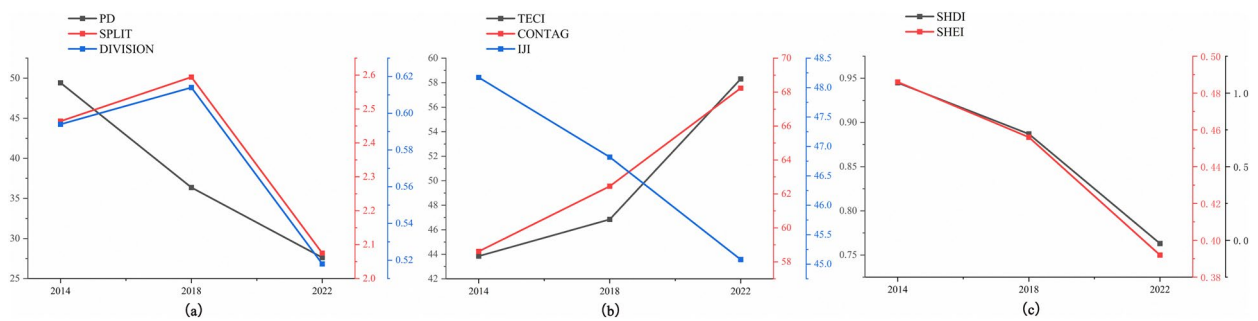

Fig. 8 Results of overall landscape pattern indices at the type level for the Shibing WHS from 2014 to 2022. **a** Presents the indices for PD, SPLIT, and DIVISION; **b** shows the indices for TECI, CONTAG, and IJI; **c** followed by SHDI and SHEI indices

Table 5 Results of landscape pattern indices for different landscape types in the Libo-Huanjiang WHS

Patch Type Level	Year	GL	CL	BL	WL	WB	UL
NP	2014	4013	4649	669	1193	302	2307
	2018	8925	7415	2569	1664	217	2353
	2022	6153	6268	1168	1254	305	738
PD	2014	4.922	5.702	0.821	1.463	0.370	2.830
	2018	10.946	9.094	3.151	2.041	0.266	2.886
	2022	7.549	7.690	1.433	1.539	0.374	0.905
LPI	2014	0.041	1.280	0.166	63.863	0.094	0.130
	2018	0.063	0.965	0.313	63.780	0.087	0.030
	2022	0.046	1.713	0.134	63.034	0.046	0.034
LSI	2014	72.907	92.663	31.513	42.487	22.207	57.868
	2018	123.595	106.548	53.802	56.019	20.492	56.828
	2022	97.214	103.729	40.117	45.184	22.412	31.424
AI	2014	53.425	75.258	68.609	95.027	62.580	68.341
	2018	52.897	67.401	57.713	93.405	67.272	52.434
	2022	50.573	72.518	59.737	94.740	56.940	63.350

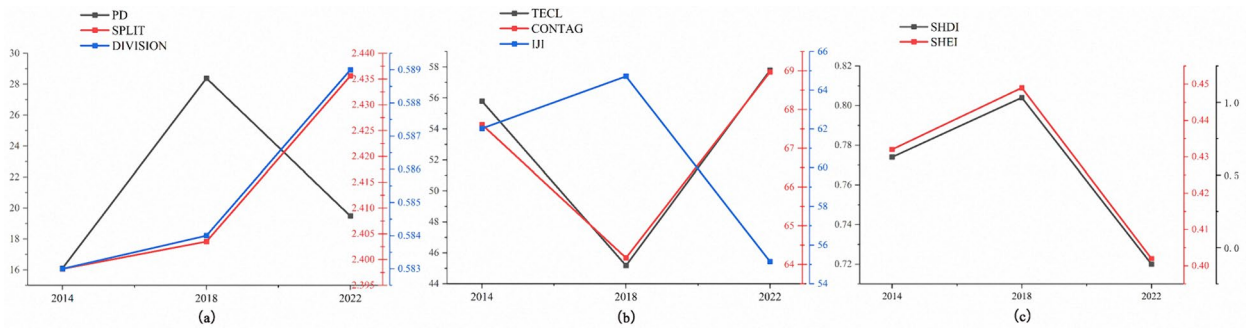

Fig. 9 Results of overall landscape pattern indices at the type level for the Libo-Huanjiang WHS from 2014 to 2022. **a** Presents the indices for PD, SPLIT, and DIVISION; **b** shows the indices for TECI, CONTAG, and IJI; **c** followed by SHDI and SHEI indices

site. From 2018 to 2022, the PD value decreased, showing a reduction in fragmentation compared to 2018. The SPLIT index has tiny values, indicating a reduced level of fragmentation, although these values are increasing. The degree of fragmentation is generally rising, taking into account both human and natural influences. Between 2014 and 2022, the landscape DIVISION index was largely steady but exhibited an increased trend. Both the TECI Index and the CONTAG Index fell and subsequently grew. The IJI Index first climbed before decreasing, indicating that the landscape was unevenly distributed between 2014 and 2018, with weak spatial connectedness and a trend toward discontinuous and discrete spatial distribution of landscape patches. However, there was an improvement between 2018 and 2022. Changes in landscape heterogeneity can be evaluated using the SHDI Index and SHEI Index. Between 2014 and 2018, both SHDI and SHEI increased gradually, indicating an increase in landscape type variety, which is advantageous to species richness. Between 2018 and 2022, both SHDI and SHEI experienced varied degrees of deterioration.

Temporal and spatial variability characteristics of landscape stability

Landscape stability is influenced by the qualities of its constituent elements and their spatial distribution patterns. Changes in the composition and spatial patterns of the landscape result in changes to landscape stability. Evaluating landscape stability in relation to landscape pattern dynamics can provide an important theoretical framework for managing and planning the WHS ecosystem.

The spatial distribution map of landscape stability (Fig. 10) demonstrates that places with reasonably intact land patches and unambiguous boundaries have better landscape stability. The distribution of landscape stability in the studied area demonstrates substantial geographic

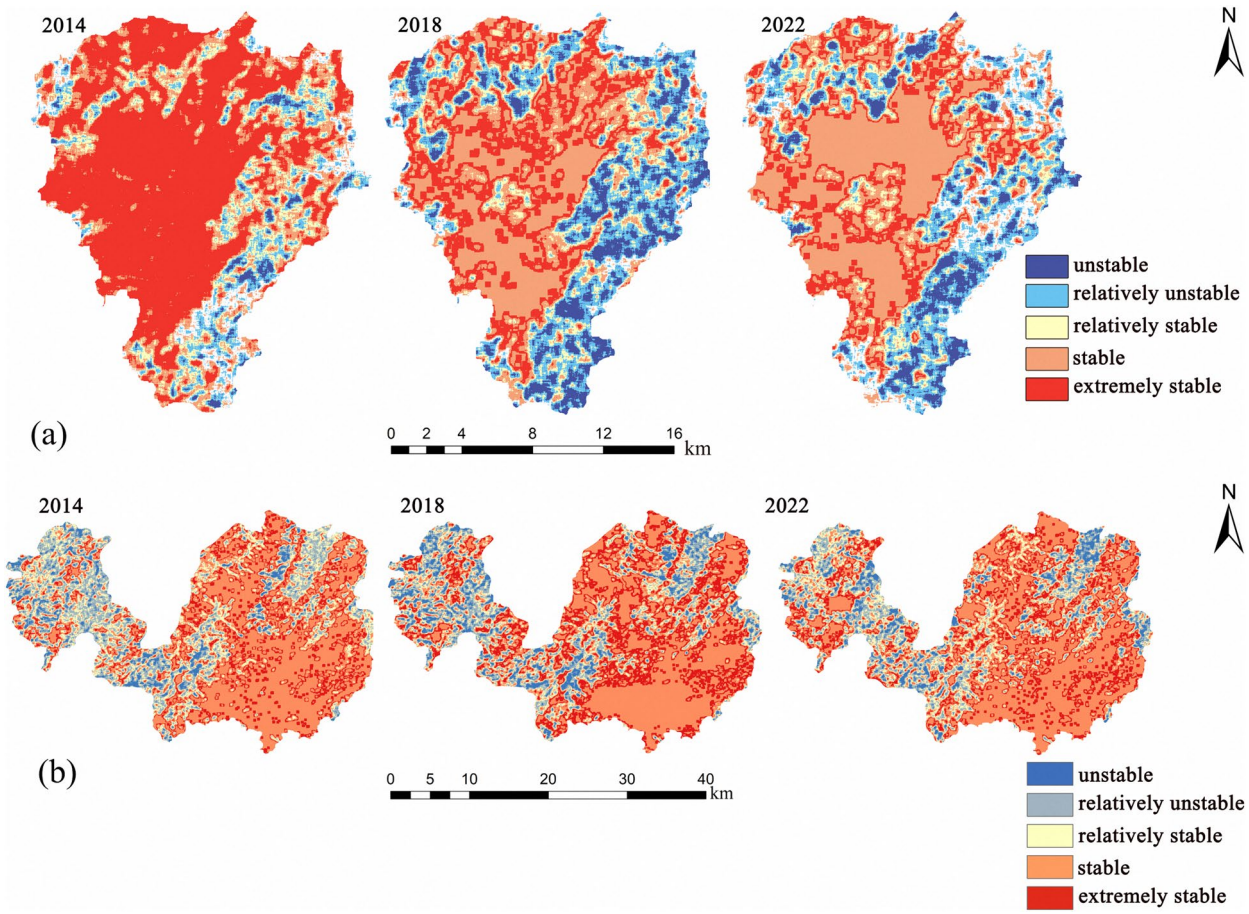

Fig. 10 Spatial distribution map of landscape stability. **a** Landscape stability distribution map of Shibing WHS; **b** landscape stability distribution map of Libo-Huanjiang WHS

differences, with stable and extremely stable areas concentrated in the core. Overlaying these locations with land use at different times and doing statistical analysis demonstrates that these areas are largely covered by WL and GL in the core zone, with minimum human intervention, strong landscape integrity, and thus superior stability. The less stable and unstable areas are primarily located in buffer zones with high human activity, such as BL and CL. The fragmentation of WL reduces patch aggregation, increases contagion, and creates more complicated boundaries, gradually lowering landscape stability. The reasonably stable areas are primarily UL and GL, where human disturbances are quite low.

Further statistical study of the area transfer features of landscape stability levels at different periods leads to the following conclusions (Fig. 11): In 2014, the Shibing Karst landscape was characterized by a rather steady level. Shibing was officially declared as a WHS in 2014, owing to its steady biological environment and optimal landscape stability. From 2018 to 2022, the landscape was mainly characterized by a stable level. Between 2014 and 2018, human and natural disruptions resulted in the shift of 88.761 km^2 from the extremely stable level, primarily to the stable level. The relatively stable level is spread over an area of 3.506 km^2. The unstable, relatively unstable, and stable levels received transferred areas of 28.009 km^2, 25.606 km^2, and 38.658 km^2, respectively. Between 2018 and 2022, 15.368 km^2 was transferred from the extremely stable level, 9.905 km^2 from the unstable level, and 4.373 km^2 from the relatively unstable level. The relatively stable and stable levels received 10.391 km^2 and 19.254 km^2, respectively.

From 2008 to 2022, the terrain at the Libo-Huanjiang WHS remained mostly stable. Between 2014 and 2018, the somewhat unstable and relatively stable levels lost 17.906 km^2 and 31.230 km^2, respectively, while the unstable and extremely stable levels gained 19.268 km^2 and 54.998 km^2, respectively. Because of human disturbance, the proportions of extremely stable and unstable levels were higher in 2018 than in previous years, demonstrating considerable landscape changes and a major impact of human disturbance on landscape stability. Between

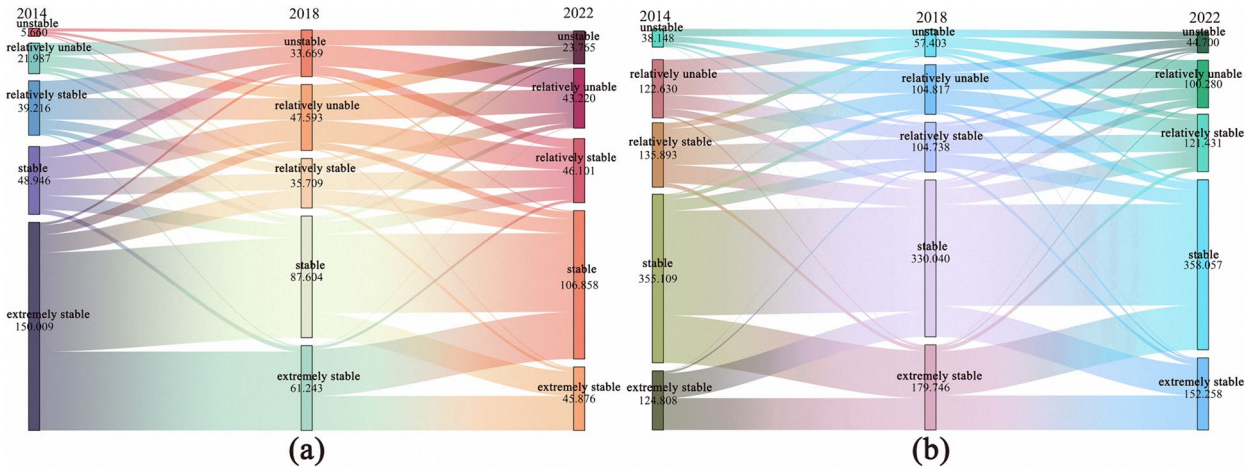

Fig. 11 Mulberry diagrams of landscape stability changes in the study areas. **a** Shibing WHS landscape stability change diagram; **b** Libo-Huanjiang WHS landscape stability change diagram

2018 and 2022, 27.528 km^2 was transferred from the extremely stable level, with transfers also occurring at the unstable and relatively unstable levels.

Landscape stability temporal heterogeneity characteristics

Spatial autocorrelation analysis

Using spatial ArcGIS Desktop 10.8 (ArcGIS 10.8) statistics tool Moran's I, a spatial autocorrelation analysis was conducted on the spatial distribution of landscape stability from 2014 to 2022. The results revealed that the global Moran's I index for the Shibing WHS in the three phases from 2014 to 2022 was 0.4409, 0.5553, and 0.5035, with Z-values of 35.2826, 42.6838, and 35.2232, respectively. The worldwide Moran's I index for the Libo-Huanjiang WHS during the same era was 0.5078, 0.5149, and 0.5044, respectively, with Z-values of 59.4068, 69.7045, and 60.3875. These findings passed the 5% significance level, demonstrating that the landscape stability in the Shibing WHS has shown spatial positive autocorrelation and considerable clustering over the last eight years. However, the Moran's I index fluctuated throughout an eight year period, with an initial gain followed by a decline and then an overall increase.

Further local spatial autocorrelation analysis revealed that in 2014, the landscape stability in the Shibing WHS had no significant clustering. In 2018 and 2022, high-high-value landscape stability clusters were primarily centered in the heritage site's core and northern sections (Fig. 12), while low-low-value clusters were clustered in the southeast. Regions with high-low value heterogeneity were intermittently dispersed. The high-high-value cluster region grew steadily from 2014 to 2022, covering 91.777 km^2 over eight years. From 2014 to 2022, the spatial clustering of landscape stability at the Libo-Huanjiang WHS was dominated by highly high-high-value clusters, which were mostly dispersed in the heritage site's core region and environs, and showed a growing trend over time. Low-low value clusters were found in the eastern section of the heritage site and gradually decreased with time.

Distribution and variability characteristics of stability hot-spots

Using the Getis-Ord G_i^* association index, a hotspot spatial distribution analysis of landscape stability in the Shibing WHS was performed for the years 2014, 2018, and 2022. The following observations were observed while considering confidence levels of 90%, 95%, and 99% for landscape stability hotspots: Over eight years, the extent of hot-spot zones in the Shibing WHS decreased first, then increased, resulting in an overall reduction. In contrast, the area of cold-spot zones followed the opposite trend. Hot and cold spot regions accounted for more than 77% of the entire research area, while non-significant regions made up more than 20%. For the Libo-Huanjiang WHS, the area of hot-spot zones decreased initially, then increased, resulting in an overall rise. In contrast, the area of non-significant regions displayed the reverse trend, while the area of cold-spot regions continued to decline.

Regarding the internal structure, both hot-spot and cold-spot zones in the Shibing WHS and Libo-Huanjiang WHS were mostly regulated within the 99% confidence interval (Fig. 13). Between 2014 and 2022, the hot-spot zones in the Shibing WHS were mostly concentrated in the core area of the heritage site, with a few distributed around the northern part. In 2014, the

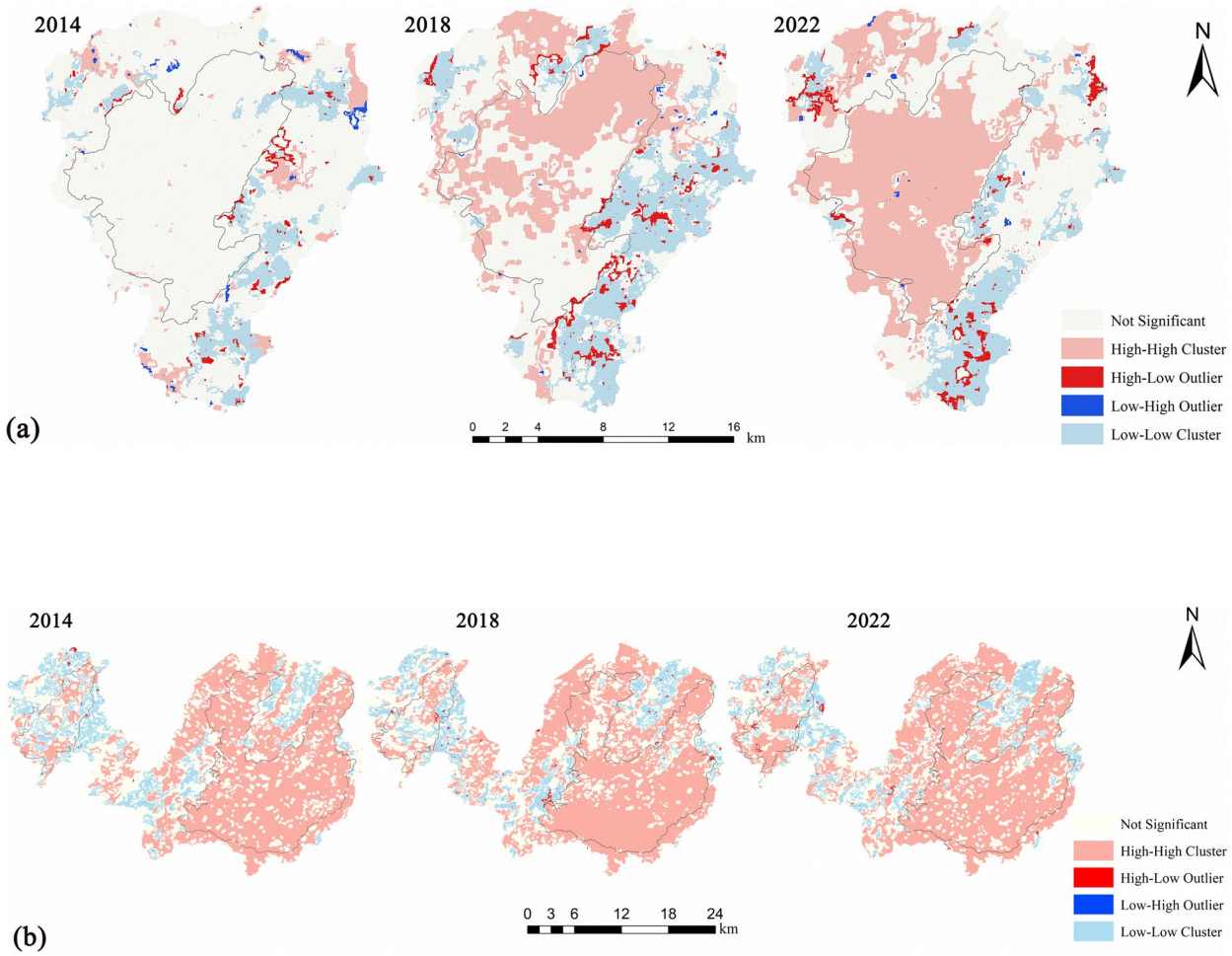

Fig. 12 Cluster and outlier of landscape stability in the study areas from 2014 to 2022. **a** Shibing WHS Cluster and Outlier; **b** Libo-Huanjiang WHS Cluster and Outlier

hot-spot regions for landscape stability covered an area of 181.794 km^2, accounting for 68.396% of the entire research area, representing the period with the greatest distribution of landscape stability hot-spot regions in the Shibing WHS over the previous eight years. Cold-spot regions in Shibing WHS were primarily found in the southeastern region, with a cold-spot size of 55.312 km^2 in 2018, accounting for 20.811% of the entire study area. In the case of the Libo-Huanjiang WHS, the hot-spot regions were primarily located in the eastern part of the heritage site, with the hot-spot area reaching its maximum in 2022, covering an area of 482.395 km^2, which was the largest during the eight years and accounted for 62.066% of the total study area. Cold-spot regions were scattered around the core area of the heritage site, with an area of 106.031 km^2 in 2014, representing the largest proportion during the eight years.

Discussion

The functionality and evolution of landscapes are influenced by the geographical variability of the landscape and the integrity of heritage assets [34]. However, considerable impacts on the direction of landscape succession have happened as a result of some unstoppable manmade factors, including changes in policy, land use, population increase, and behaviors like mining, pollution, and settlement [35]. Furthermore, the degree of landscape stability in the research area has steadily decreased due to the fragmentation of karst background landscapes. The central dispute at now about the integrity of natural heritage is whether sustainable development and conservation can coexist. The preservation of landscape stability is a crucial step in safeguarding the integrity of heritage sites, which in turn depends on the integrity of natural sites. The two go hand in hand and make up the foundation of managing and protecting natural assets. The factors influencing the integrity of WHSs are mainly analyzed from

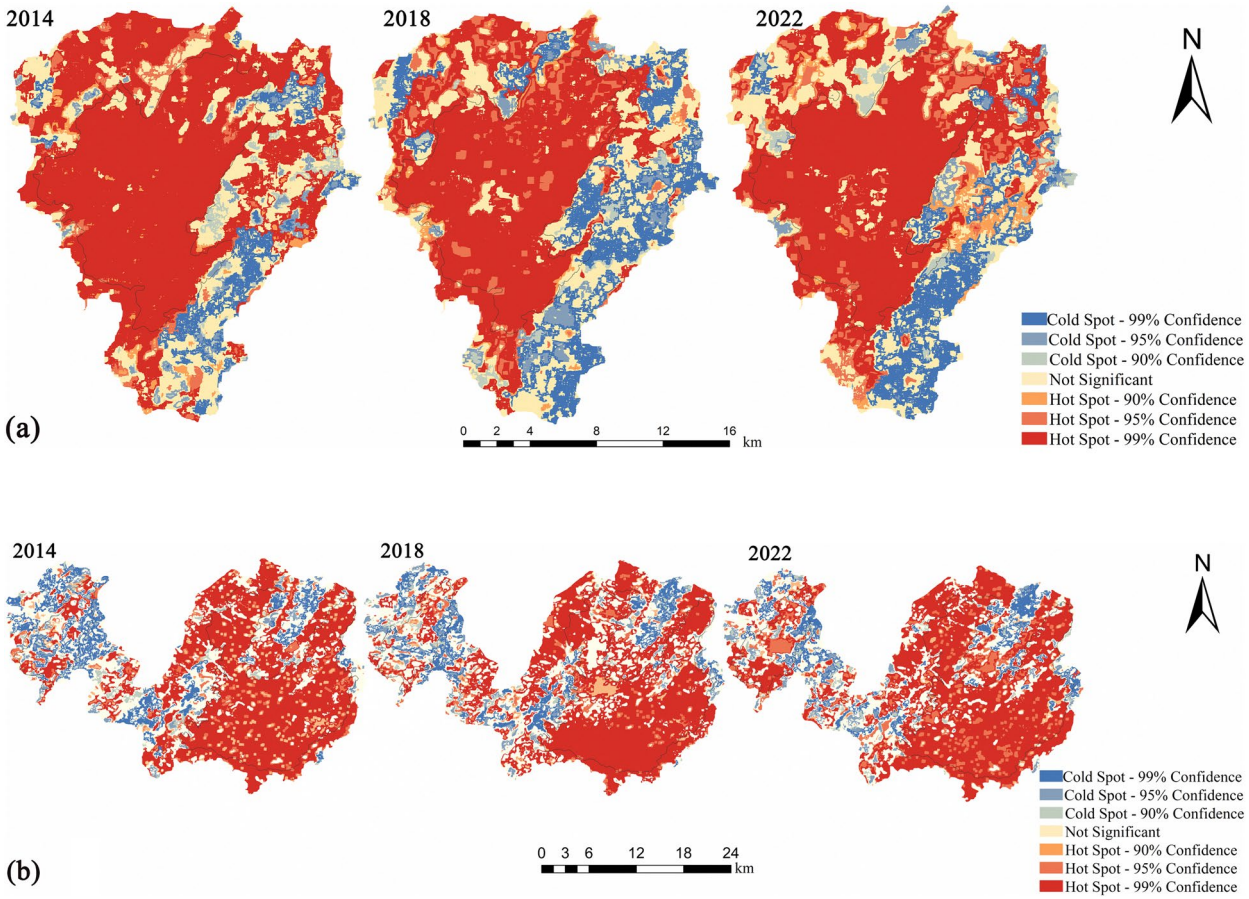

Fig. 13 Landscape stability cold-spots and hot-spots spatiotemporal variations from 2014 to 2022 in the Study Areas from 2014 to 2022. (**a**) Shibing WHS cold-spots and hot-spots spatiotemporal variations; (**b**) Libo-Huanjiang WHS cold-spots and hot-spots spatiotemporal variations

four aspects: first, the components, mainly referring to the reduction or disappearance of biodiversity and heritage elements; second, the scale of heritage sites, involving boundary planning and the protection of site integrity, including the loss or destruction of landscape connectivity, key areas, and routes; third, ecosystems, mainly referring to biological ecological processes and relationships, emphasizing a systemic and holistic perspective; finally, feature transformation, mainly referring to the transformation of the original natural landscape pattern and land use nature of heritage sites, including changes in vegetation patterns, river course alterations, and human activities [36–38]. These elements have a direct impact on heritage sites' biological services as well as landscape stability. In-depth examination of these impacting elements is critical for developing successful solutions for sustainable development and protection.

Landscape stability is primarily influenced by factors such as internal ecosystem structure (biodiversity, nutrient structure, community structure, invasive species) [39], landscape heterogeneity [40], soil quality and erosion [41], natural disasters [42, 43], and human interference [36, 38] (Fig. 14). SCK landscapes are formed by soluble rocks, and soil erosion may exacerbate soil erosion and lead to the destruction of surface and subsurface cave systems, altering the original landscape features. Severe precipitation events raise the possibility of soil erosion. In addition to having an impact on plant development, this could cause unique landscape types like karst topography to deteriorate [44]. Natural disasters and human activities have a diverse impact on landscape stability, worsening the degree of fragmentation to varying degrees and thereby affecting landscape stability [45, 46]. This study indicates that relatively concentrated landscape patches with good patch integrity and strong connectivity contribute to enhancing overall landscape stability. Between 2014 and 2022, there was a noticeable difference in landscape stability between the core area and buffer zone of WHSs. The presence of buffer zones aims to protect the geomorphological value of WHSs from threats. The buffer zones are mainly dominated by

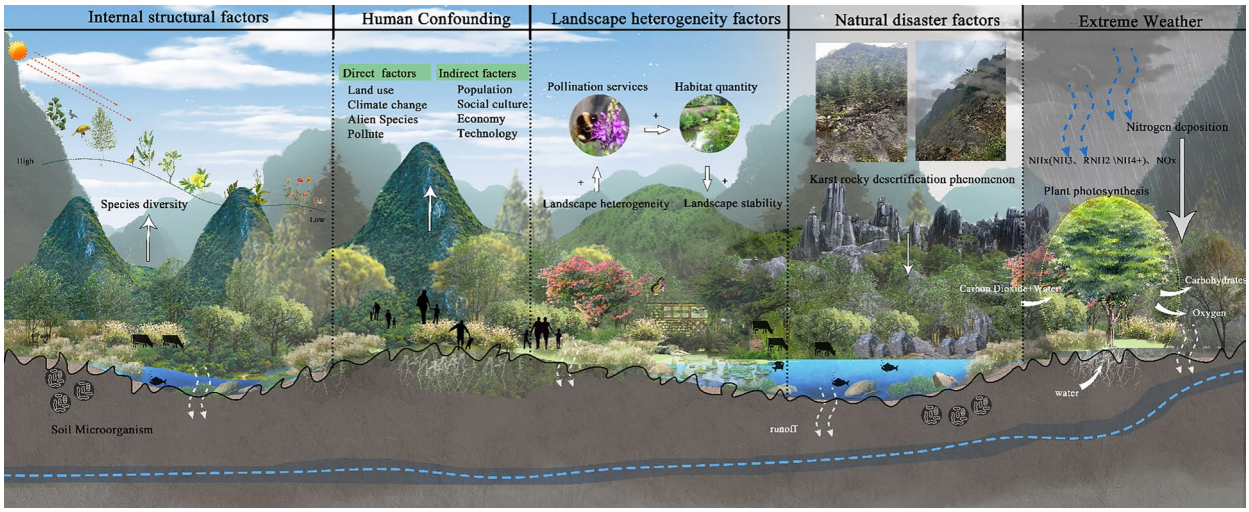

Fig. 14 The factors influencing landscape stability primarily include internal factors, human activities, landscape heterogeneity, natural disasters, and extreme weather events

cultivated land and construction land, leading to high levels of landscape fragmentation and poor landscape stability [46]. In contrast, the core areas are primarily dominated by forest landscapes, exhibiting better landscape stability. Additionally, traditional production and settlement activities have continued and complex impacts on landscape structure. For example, concerns like agricultural runoff and sewage treatment in the Shibing Karst area endanger water quality and the geomorphological significance of heritage sites. The construction of the "Guinan Railway" infrastructure in 2016 significantly affected the landscape stability of the Libo-Huanjiang Karst area, resulting in increased landscape fragmentation and the dispersal of landscape patches, thereby reducing the landscape stability of the buffer zone. Although the high-speed rail project attempts to maintain the sites' outward significance, it may have some environmental implications within the buffer zone. Despite the fact that rigorous precautions have been put in place to prevent the introduction of new invasive species into the site, the buffer zone's potential environmental implications still need to be assessed [47–50].Tourism development has had the most significant impact on the Shibing and Libo-Huanjiang Karst zones. Most WHSs possess high-quality tourism resources, providing a solid material foundation for local tourism development and economic growth. While tourism activities promote economic development, they also have a negative impact on the landscape stability of heritage sites [51, 52]. Tourism exerts a predominantly short-term, pronounced, and episodic impact on landscapes, contrasting with the gradual, long-term effects that natural elements have on shaping the landscape's configuration [53].

To reduce the direct introduction of tourism pollutants into natural regions, protection measures such as wastewater interception and treatment, river cleaning, and continual maintenance and monitoring have been implemented [53–56]. Monitoring efforts are undertaken by satellite remote sensing, observation station observations, instrument monitoring, and community patrols to collect data on threats to the World Tourism Organization, the environment, and tourist numbers [50]. Appropriate-scale development and landscape protection are not incompatible. To ensure that tourism promotion does not exacerbate the negative impacts on heritage sites, it is necessary to establish relevant laws and regulations, strictly control tourism development activities, and strike a balance between appropriate-scale development and landscape protection [56]. These strategies can help to reduce the detrimental impact of human activities on the landscape stability of the heritage site, while simultaneously supporting long-term economic development. To ensure the heritage site's long-term stability, it is critical to regularly monitor and analyze the impact of these operations, as well as alter management techniques depending on the data acquired.

Conclusions

Due to its distinct geological and climatic past, the SCK has generated distinct ecosystems and biodiversity as well as a range of geomorphological forms. In recent years, the protection of WHSs has received particular attention. The way that land is used inside these WHSs

is changing, and safeguarding and making use of Karst WHSs continues to be a major area of research and a long-term challenge in World Heritage conservation and usage. For national development, it is crucial to strike a balance between ecological preservation and economic development in WHSs. The study, focusing on the Shibing and Libo-Huanjiang WHSs within SCK region, utilized landscape pattern indices and the Moran's I index system to investigate the spatiotemporal distribution changes and heterogeneity characteristics of land use over the past eight years. The following primary conclusions were drawn:

WL coverage has the most significant impact on both Shibing and Libo-Huanjiang WHSs, with a steady increase in the percentage of WL, indicating good landscape stability. This underscores the importance of maintaining and enhancing forest ecosystems within the protected areas.

GL and CL in both WHSs exhibit high NP, PD, and LSI values, reflecting significant spatial heterogeneity and irregular shapes of peripheral patches, which increases complexity. This suggests that landscape management in these areas should focus on biodiversity conservation and preventing land degradation.

Over the past eight years, the overall landscape index changes for the Shibing WHS have shown a steady decline in PD, IJI, SHDI, and SHEI, indicating a reduction in landscape heterogeneity, diversity, and fragmentation, while TECL and CONTAG have steadily increased, signaling an improvement in landscape aggregation. For the Libo-Huanjiang WHS, after an initial phase of human disturbance affecting landscape fragmentation, diversity, heterogeneity, and aggregation, landscape trends have improved compared to 2014, demonstrating adaptability and recovery from disturbance.

Most of the studied area maintains a relatively stable landscape concerning changes in landscape pattern stability, despite significant alterations in both the core and buffer zones due to economic activities. Although there is greater landscape stability in the core areas, the degree of anthropogenic modification varies significantly among them.

The Shibing and Libo-Huanjiang WHSs display spatial clustering of landscape stability, mainly characterized by high-high-value clustering. The areas for hot spots and cold spots are primarily located in the central regions of the heritage sites, governed by a 99% confidence interval.

These findings highlight the importance of balancing ecological conservation with economic development within Karst WHSs. The results provide a basis for formulating scientific management strategies aimed at promoting the long-term protection and sustainable utilization of these areas.

Abbreviations

WHS	World heritage site
SCK	South China Karst
CL	Cultivated land
GL	Grassland
WL	Woodland
WB	Waterbody
BL	Build-up land
UL	Unused land

Author contributions

Conceptualization: KX, XB; methodology: XB; data collection and analysis: XB; writing—original draft: XB; writing—review and editing: KX, XB; supervision: YC, ZQ; funding acquisition: KX. All authors read and approved the final manuscript.

Funding

This research was supported by the Guizhou Provincial Key Technology R&D Program (No. 220 2023 QKHZC), the Key Project of Science and Technology Program of Guizhou Province (No. 5411 2017 QKHPTRC), and China Overseas Expertise Introduction Program for Discipline Innovation (No. D17016).

Data availability

Data are available from the authors upon request.

Declarations

Competing interests

The authors declare no competing interests.

Received: 5 March 2024 Accepted: 14 June 2024
Published online: 24 June 2024

References

1. Prokopová M, Salvati L, Egidi G, Cudlín O, Včeláková R, Plch R, Cudlín P. Envisioning present and future land-use change under varying ecological regimes and their influence on landscape stability. Sustainability. 2019;11:4654.
2. Ives AR, Carpenter SR. Stability and diversity of ecosystems. Science. 2007;317:58–62.
3. Zhang Y, Zhang H. Evaluating landscape stability through disturbance regimes in Zhalong Wetland, China. Ekoloji. 2019;28(107):2005–11.
4. Frondoni R, Mollo B, Capotorti G. A landscape analysis of land cover change in the municipality of Rome (Italy): spatio-temporal characteristics and ecological implications of land cover transition from 1954 to 2001. Landsc Urban Plan. 2011;100:117–28.
5. Tian P, Cao LD, Li JL, Pu RL, Liu YC, Zhang HT, Wang CY. Ecosystem stability assessment of Yancheng coastal wetlands, a world natural heritage site. Land. 2022;11:564.
6. Li H, Guo WQ, Liu Y, Zhang QM, Xu Q, Wang ST, Huang X, Xu KX, Wang JZ, Huang YL, Gao W. The delineation and ecological connectivity of the three parallel rivers natural world heritage site. Biology. 2023;12:3.
7. Peng B, Yang J, Li Y, Zhang S. Land-use optimization based on ecological security pattern—a case study of Baicheng, Northeast China. Remote Sens. 2023;15:5671.
8. Hermosilla T, Michael AW, Joanne CW, Nicholas CC, Paul DP, Douglas KB. Impact of time on interpretations of forest fragmentation: three-decades of fragmentation dynamics over Canada. Remote Sens Environ. 2018;2019(222):65–77.
9. Yu KJ, Li DH. Landscape design: profession, discipline, and education. Beijing: China Architecture & Building Press; 2003. p. 79–93 (**in Chinese**).
10. Kang SL, Yue BR. The method of landscape spatial pattern optimization based on coupling mechanism of patterns and processes. Chin Landsc Arch. 2017;33(03):50–5 (**in Chinese**).
11. Plieninger T, Kizos T, Bieling C, Dû-Blayo LL, Budniok MA, Bürgi M, Crumley CL, Girod G, Howard P, Kolen J, Kuemmerle T, Milcinski G, Palang H, Trommler K, Verburg PH. Exploring ecosystem-change and

society through a landscape lens: recent progress in European landscape research. Ecol Soc. 2015;20(2):5.
12. Zhang YH, Su LY, Yu WH, Zhang HY. Landscape ecology—pattern, processing, scale and hierarchy. Beijing: Advanced Education Press; 2000. (**in Chinese**).
13. Zhang ZH, Wang XT, Zhang Y, Gao Y, Liu YX, Sun XM, Zhi JJ, Yin SF. Simulating land use change for sustainable land management in rapid urbanization regions: a case study of the Yangtze River Delta region. Landsc Ecol. 2023;38:1807–30.
14. Zhang M, Xiong K, Wang X, Zhao X. Natural beauty and esthetic value of natural world heritage sites: a literature review and implications for Karst Geoheritage Sites. Geoheritage. 2022;14(3):1–13.
15. Xiong KN, Li GC, Wang YL. Study on the protection and sustainable development of South China Karst Libo World Natural Heritage Site. Chin Landsc Arch. 2012;28(08):66–71.
16. UNESCO (1972) Convention Concerning the Protection of the World Cultural and Natural Heritage. Paris: UNESCO World Heritage Centre
17. Florida S, Williams PW (2007) World Heritage caves and karst: a thematic study. IUCN
18. IUCN (2007) Evaluation of nominations of natural and mix properties to the Word Heritage List, Christchurch, New Zealand
19. Zhang X, Wang ZJ. Evaluation and characteristic analysis of urban landscape stability in karst mountainous cities in the central Guizhou Province. Acta Ecol Sin. 2022;42(13):5243–54 (**in Chinese**).
20. Hu CY, Wu W, Zhou XX, Wang ZJ. Spatiotemporal changes in landscape patterns in Karst mountainous regions based on the optimal landscape scale: a case study of Guiyang City in Guizhou Province, China. Ecol Indic. 2023. https://doi.org/10.1016/j.ecolind.2023.110211.
21. Xu QY, Wang WW, Mo L. Evaluation of landscape stability in Beijing-Tianjin-Hebei region. Acta Ecol Sin. 2018;38(12):4226–33 (**in Chinese**).
22. Zhang XJ, Wang GQ, Xue BL, Zhang MX, Tan ZX. Dynamic landscapes and the driving forces in the Yellow River Delta wetland region in the past four decades. Sci Total Environ. 2021;787: 147644.
23. Zeng CF, He J, He QQ, Mao YQ, Yu BY. Assessment of land use pattern and landscape ecological risk in the Chengdu-Chongqing economic circle, Southwestern China. Land. 2022;11(5):659.
24. Tarr NM. Demonstrating a conceptual model for multispecies landscape pattern indices in landscape conservation. Landscape Ecol. 2019;34:2133–47.
25. Zhang Q, Chen CL, Wang JZ, Yang DY, Zhang YE, Wang ZF, Gao M. The spatial granularity effect, changing landscape patterns, and suitable landscape metrics in the Three Gorges Reservoir Area, 1995–2015. Ecol Ind. 2019;2020(114): 106259.
26. Wei HJ, Yang YM, Xiong GC, Cao YY. Study on landscape pattern and ecosystem services in Luanchuan County, upper reaches of the Yi River Basin. Henan Sci. 2021;39:1298–309.
27. Wang ZQ, Cao SH, Zhou YH, Cao XT, Gao Y, Liu XZ. Spatial and temporal characteristics of landscape pattern dynamics and stability in Liuyang River Basin in recent three decades. J Yangtze River Sci Res Inst. 2021;38(09):64–70 (**in Chinese**).
28. Zhang LL, Zhao YH, Yin S, Fang S, Liu XJ, Pu MM. Gradient analysis of dry valley of Minjiang River landscape pattern, based on moving window method. Acta Ecol Sin. 2014;34(12):3276–84 (**in Chinese**).
29. Lv LT, Zhang J, Peng QZ, Ren FP, Jiang Y. Landscape pattern analysis and prediction in the Dongjiang River Basin. Acta Ecol Sin. 2019;39(18):6850–9 (**in Chinese**).
30. Ding Q, Wang L, Fu MC, Huang N. An integrated system for rapid assessment of ecological quality based on remote sensing data. Environ Sci Pollut Res. 2020;27(26):32779–95.
31. Ren HR, Shang YJ, Zhang S. Measuring the spatiotemporal variations of vegetation net primary productivity in Inner Mongolia using spatial autocorrelation. Ecol Ind. 2020;112(79): 106108.
32. Gao J, Li T, Jia BQ, Zhang QM, Liu WR. Ecological land and its spatial stability analysis-Taking Xianyang City as an example. Acta Ecol Sin. 2020;42(23):9843–56 (**in Chinese**).
33. Shi H, Yang ZP, Han F, Shi TG, Li D. Assessing landscape ecological risk for a world natural heritage site: a case study of Bayanbulak in China. Polish J Environ Stud. 2015;24(1):269–83.
34. Xiong KN, Chen D, Zhang J, Gu XY, Zhang N. Synergy and regulation of the South China Karst WH site integrity protection and the buffer zone agroforestry development. Herit Sci. 2023;11:218.
35. Chen Z, Deng XZ, Yang J, Cheng YJ, Zhao TX, Wang PR. The exploration of residents' perception of eco-urbanization at community and driving factors in China. Cities. 2022;122: 103513.
36. Wan LH, Zhang YW, Zhang XY, Qi SQ, Na XD. Comparison of land use/land cover change and landscape patterns in Honghe National Nature Reserve and the surrounding Jiansanjiang Region, China. Ecol Indic. 2015;51:205–14.
37. Wei ZD, Du N, Yu WZ. Land use change and its driving factors in the ecological function area: a case study in the Hedong Region of the Gansu Province, China. J Arid Land. 2024;16:71–90.
38. Jiang L, Pu ZC. Different effects of species diversity on temporal stability in single-trophic and multitrophic communities. Am Nat. 2009;174(5):651–9.
39. Amparo L, Alomar D. Landscape heterogeneity increases the spatial stability of pollination services to almond trees through the stability of pollinator visits. Agric Ecosyst Environ. 2019;279:149–55.
40. Wang YF, Jiang LL, Wang ZZ, Song MH, Wang SP. Phosphorus enrichment increased community stability by increasing asynchrony and dominant species stability in Alpine Meadow of Qinghai-Tibet Plateau. J Geophys Res Biogeosci. 2022. https://doi.org/10.1029/2022JG006819.
41. Evans LC, Melero Y, Schmucki R, Boersch-Supan PH, Brotons L, Fontaine C, Jiguet F, Kuussaari M, Massimino D, Robinson RA, Roy DB, Schweiger O, Settele J, Stefanescu C, van Turnhout CA, Oliver TH. Bioclimatic context of species' populations determines community stability. Glob Ecol Biogeogr. 2022;31:1542–55.
42. Toby Kiers E, Todd MP, Anthony RI, John FB, Judith LB. Mutualisms in a changing world: an evolutionary perspective. Ecol Lett. 2010;13(12):1459–74.
43. Kammerbauer J, Ardon C. Land use dynamics and landscape change pattern in a typical watershed in the hillside region of central Honduras. Agric Ecosyst Environ. 1999;75(1/2):93–100.
44. Chen HS, Feng T, Li CZ, Fu ZY, Lian JJ, Wang KL. Characteristics of soil erosion in the Karst regions of Southwest China: research advance and prospective. J Soil Water Conserv. 2018;32(1):10–6 (**in Chinese**).
45. Southworth J, Munroe D, Nagendra H. Land cover change and landscape fragmentation—comparing the utility of continuous and discrete analyses for a western Honduras region. Agric Ecosyst Environ. 2004;101(2/3):185–205.
46. Zhang J, Xiong KN, Liu ZJ, He ZJ, Zhang N, Gu XY, Chen D. Exploring the synergy between Karst World Heritage site's OUV conservation and buffer zone's tourism industry development: a case study of the Libo-Huanjiang Karst. Herit Sci. 2023;11:202.
47. Xiong KN, Zhang ZZ, Xiao SZ, Di YN, Xiao H, Zhang Y, Zhang Y, Liu SX. Impact of Guinan Railway Construction on the Geomorphologic Value of the Libo-Huanjiang Karst World Heritage Site. Trop Geogr. 2020;40(3):466–77.
48. UNESCO (2015) Managing natural world heritage (world heritage resource manual). Paris: UNESCO
49. UNESCO (2021) Operational guidelines for the implementation of the world heritage convention. Paris: UNESCO
50. Sun J, Wu ZB, Zheng GY. Study on the case of environmental protection route selection in railway construction project—a case study of Guiyang-Nanning Railway Project in the Libo World Natural Heritage Site in Guizhou Province. J Railway Energy Conserv Environ Protect. 2017;7(01):5–8 (**in Chinese**).
51. World Heritage Committee. Decision 43COM 7B.4. South China Karst (China). In: Report of decisions of the 43rd session of the World Heritage Committee (Baku, Azerbaijan, 2019). Paris, France: UNESCO World Heritage Centre. Available at: https://whc.unesco.org/en/decisions/7434. Accessed 6 Nov 2020
52. IUCN. World Heritage Nomination—IUCN Technical Evaluation, South China Karst (China). In: IUCN World Heritage Evaluations 2007, IUCN Evaluations of nominations of natural and mixed properties to the World Heritage List. WHC/06/30.COM Gland, Switzerland: IUCN. https://whc.unesco.org/en/list/1248/documents/. Accessed 25 Nov 2020
53. Xu LL, Yu X, Zhong LS. Evolution of the landscape pattern in the Xin'an River Basin and its response to tourism activities. Sci Total Environ. 2023;880: 163472.
54. IUCN (2020) World heritage advice note: environmental assessment. www.iucn.org/worldheritage

55. South China Karst—2020 Conservation Outlook Assessment. IUCN World Heritage Outlook: https://worldheritageoutlook.iucn.org/
56. Wang HT. Study on conservation and tourism planning of world natural heritage site in Jinfoshan Karst. J Herit Protect China. 2017;2(01):39–44.

Publisher's Note